SPE-175020-MS

Interpretation of Real-Time Pressure Measurements to Detect CO2 Leakage

S. Alireza Haghighat, Eclipse Resources; Shahab D. Mohaghegh, West Virginia University

This paper was prepared for presentation at the SPE Annual Technical Conference and Exhibition held in Houston, Texas, USA, 28–30 September 2015.

Abstract

Carbon Capture and Storage (CCS) has been gaining support and popularity as one of the most viable CO_2 emission mitigation methods. In order to assure underground CO_2 storage safety and reduce leakage risk, different CO_2 Monitoring techniques must be utilized. In-zone reservoir pressure, which is transmitted by Permanent Down-hole Gauges (PDG), is a widely used monitoring parameter that can provide important indications when CO_2 migration/Leakage occurs. As part of a monitoring package, a Real-Time Intelligent CO_2 Leakage Detection System (RT-ILDS) was developed for CO_2 storage project at Citronelle Dome, Alabama. This system, which is designed based on Pattern Recognition Technology and Smart Wells, is able to identify the location and amount of the CO_2 leakage at the reservoir level using real-time pressure data from PDGs.

In this work, History matched reservoir simulation model (based on 11 months of actual injection/pressure data) was used for CO_2 leakage modeling study. High frequency real time pressure streams were processed with a novel technique to form a new data driven RT-ILDS which was able to detect leakage characteristics in a short time(less than a day). RT- ILDS also demonstrated high precision in quantifying leakage characteristics subject to complex rate behaviors. Finally the performance of ILDS was examined under different conditions as multiple well leakage, availability of additional monitoring well, uncertainty in the reservoir model, CO_2 leakage through the cap rock and multi-well leakage.

The objective of this study was to proof the concept and feasibility of using real time pressure data from PDGs in order to notice occurrence of leakage and identify its characteristics as location and rate in a real CO_2 storage project by utilizing AI & DM techniques.

Introduction

Confinement of injected CO_2 in an underground storage should be secured for a long period of time. If leakage from a geological CO_2 sequestration site occurs, it is advantageous to find the approximate amount and the location of the leak, in a timely manner, in order to initiate proper remedial activities.

The leakage can have harmful ecological effects such as risks for human health and global warming. For the long term CO_2 storage, it is necessary for the target reservoir to be sealed by the impervious cap rock. Under unfavorable conditions, the integrity of the cap rock can be damaged by the inappropriately cemented wells, faults and fractures. Therefore monitoring systems must be utilized on underground storage sites to assure the cap rock's integrity. There are several monitoring techniques that can be implemented on the geological storages based on the site infra-structure, CO_2 injection program and duration of project [3]. With each monitoring system, a specific parameter is being measured continuously

or periodically in order to indicate the possible leakage. Usually these parameters are formation or reservoir pressure, formation temperature, resistivity, seismic velocity, multi frequency EM data and CO_2 concentration [6]. Research and development for storage site monitoring has been concentrated on atmospheric, surface or near surface monitoring of the sequestered CO_2. In the event of leakage in a geological CO_2 sequestration site, the CO_2 will move at the reservoir level before it can reach the surface.

Permanent Down-hole Gauges (PDGs) monitor the pressure changes in the formation and transmit high frequency data streams to the surface. The pressure changes in the reservoir are indications of fluid flow in the formation which can be caused by leak in the reservoir. CO_2 leakage detection in storage sites using pressure data from PDGs is a fairly new topic in CO_2 sequestration research area. Several authors [1][2] [7][13][15][16] tried to investigate this topic with different methodologies. Generally, most of the presented methods attempted to use analytical solutions to find pressure behavior subject to CO_2 leakage characteristic and solve the inverse problem to find leakage components [13][16] . The other methodology which was introduced by Jalali *et al* [7*]*, considered neural networks to find seepage in a CO_2 sequestration model in coal bed with multiple sensors (PDGs). All mentioned studies used synthetic models which were completely homogenous with at most two reservoir layers. The significance of the current study over previous works is usage of a history matched reservoir simulation model developed for real CO_2 sequestration project (Citronelle Field). Additionally, CO_2 leakage was detected based on a novel data processing method, implemented for analysis of real time pressure data. Finally, the robustness of our proposed method and workflow was evaluated by considering various reservoir and CO_2 leakage characteristics.

Prodecure

A reservoir simulation model for the CO_2 sequestration can be developed to assist in the leakage detection. Multiple scenarios of CO_2 leakages based on different locations and rates can be modeled to simulate high frequency pressure data from PDGs installed in the observation well. PDG data can be collected to help accommodate CO_2 leak detection. Real-time processing of high frequency pressure signals is done by data summarization methods and pattern recognition techniques. This data can be streamed in real-time while being stored in data histories. Processed data are used to build and intelligent system that relates each pressure signal to CO_2 leakage characteristic. Successful detection of location and amount of CO_2 leaking from the reservoir using the real-time data streams demonstrates the power of pattern recognition and machine learning as a reservoir and operational management tool for smart fields.

A four-step procedure can be used to accomplish this. First, a base reservoir model can be developed for a CO_2 sequestration site such as, e.g., the Citronelle Dome in Alabama. Second, actual field data (CO_2 injection rate/Down-hole pressure) can be used to history match the base model. Third, multiple leakage scenarios can be generated using the history matched reservoir model and collection of the high frequency pressure signals that result from the imposed leakage in the system. Finally, the high frequency pressure signals can be processed and analyzed using machine learning and pattern recognition technology in order to identify the location and the amount of the leakage in the system.

As an example, a reservoir model for the Citronelle saline aquifer of the Citronelle field, a saline aquifer reservoir, located in the state of Alabama was developed and history matched with real field data [4][5]. Structural maps for 17 sand layers (the most extensive ones that were targeted for CO_2 injection) were generated by interpretation and correlation of 14 well logs. Based on the correlation between the wells, 17 top maps were generated representing the lateral heterogeneity in the reservoir. The same well logs were used to generate thickness (isopach) maps for the layers. In order to make porosity maps, 40 well logs were analyzed and interpreted. Three different porosity maps were generated for each sand layer (for a total of 51 total porosity maps for the entire reservoir). Permeability of the reservoir was obtained using porosity-permeability correlations from core analysis.

In the Citronelle field, two PDGs were installed at the depths of 9416 and 9441 ft. in an observation well (D-9-8#2) which is 833 ft. away from the injection well (D-9-7#2, Figure 1a). CO_2 Injection started on August 2012 and reached to 9MMcf by end of September 2012 and continued with a flat trend until August 2013 with some periodic shut downs (Figure 1b).In the reservoir simulation model, the actual injection rate was set as operational constrain. The pressure data from PDGs were recorded at every minute through injection period and was averaged over each day. A reasonable match between actual field PDG pressure data and model's pressure at observation well was achieved by tuning brine density, permeability, vertical to horizontal permeability ratio, CO_2 solubility in brine and reservoir volume [5]. The history matched reservoir simulation model was validated by predicting pressure for the last three months of injection which was not used during history matching process. The results of history matching and model's validation are shown in Figure 2.

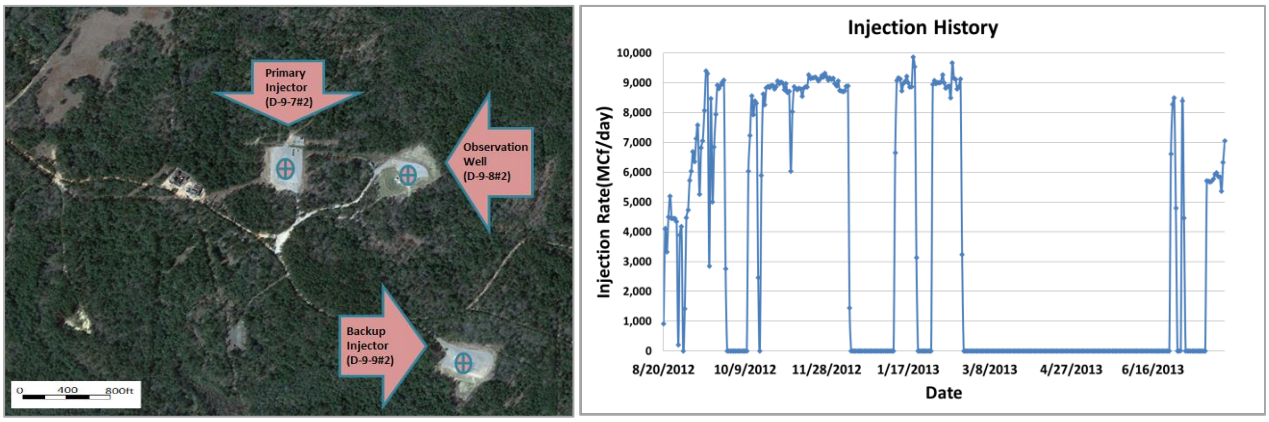

Figure 1: a) Locations of the CO_2 injection and observation wells in Citronelle Dome *b) CO_2 injection rate history*

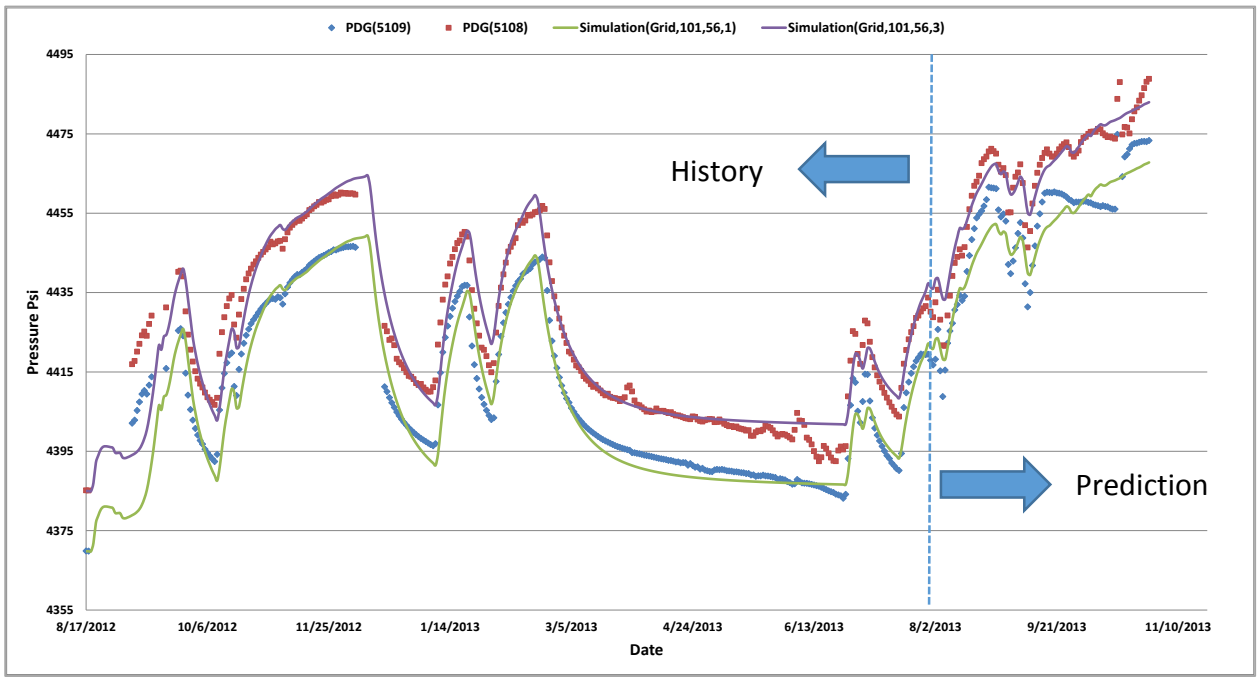

Figure 2: Model's pressure result and actual data for prediction and history

Real-Time Intelligent Leakage Detection System (RT-ILDS)

A real-time intelligent leakage detection system (RT-ILDS) is a data driven monitoring package which receives real time pressure data and determines the occurrence of CO_2 leakage, and estimates the location and amount of the leakage. This system originally was designed to receive pressure signals for a time interval, for example, one week of hourly signals or 168 records after the leakage. Summarized pressure data obtained by descriptive statistics can be fed into trained neural networks to find leakage characteristics [6]. In RT-ILDS, the pressure data can be analyzed in real-time considering the previous trend of the signals. By this method it is possible to determine leakage characteristics in less than a day.

In the area of interest which is CO_2 plume extension, five different wells are located (Figure 3.a). Each well will be prone to the leakage if the proper well integrity is not achieved. Since wells D-9-7#2 (injection well) and D-9-8#2 (observation well) were drilled in recent times specifically for CO_2 storage purposes, CO_2 leakage through these wells is considered to be improbable. Wells D-9-6, D-9-7 and D-9-8 may experience some kind of leakage. When a leakage happens, a pressure change (Δp) signal can be observed in the observation well. The pressure change signal in the observation well for the leakage rate of 65,000Cf/day, at well D-9-7 is illustrated in Figure 3.b.

In order to process the data and convert it to a format which is appropriate for the pattern recognition technology, pressure signals based on thirty different CO_2 leakage scenarios were used. Each scenario corresponded to a simulation run that modeled a specific CO_2 leakage rates ranging from 15 to 105 Mcf/day with 10 Mcf/day increments at one of the three leakage locations; wells D-9-6, D-9-7, and D-9-8.

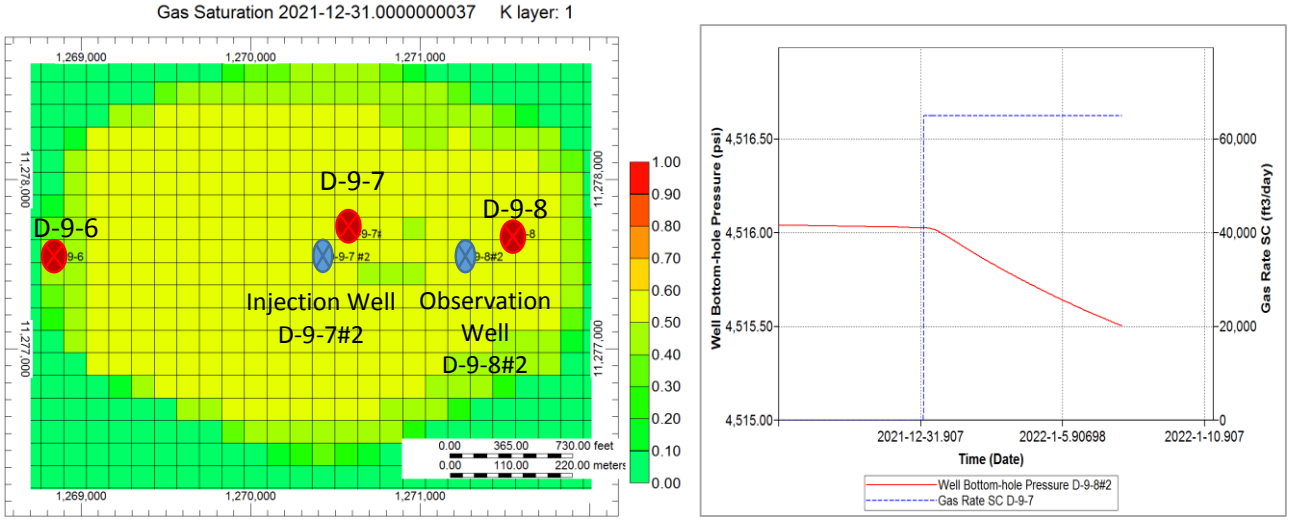

Figure 3: a) Location of five wells in the CO_2 plume area *b) Reservoir Pressure in the observation well (D-9- 8 #2) for the leakage rate of 65,000Cf/day, at well D-9-7*

A threshold was assigned as 0.01 psi for the ΔP ($P_{No\ Leakage} - P_{Leakage}$), as the leakage indicator. This threshold is actually equal to the precision of the PDGs that are currently used in the industry and that are currently installed in the observation well D-9-8#2. When this threshold is achieved, data processing starts by considering values of ΔP, pressure derivative, ΔP average, ΔP summation, ΔP standard deviation, ΔP skewness, and kurtosis for the past history of the data in a given window of time. The hourly pressure data for one week for each CO_2 leakage scenario were used to generate the data set for the neural network training. The first 12 hours of the data after beginning of the leakage ($\Delta P > 0.01$ psi) were neglected from the data processing.

Development of the RT-ILDS was mainly based on the training, calibration and verification of the neural networks that received the pre-processed real-time pressure data for each CO_2 leakage scenario as the input and the corresponding leak rate and location as the output. Initially, a neural network was

trained to find a pattern between leakage location (output) and the corresponding pre-processed pressure signals. The entire data set for leakage location neural network included 3,527 data records (ΔP at each hour) which were partitioned into 2821, 353, and 353 records for training, calibration, and verification, respectively.

The influence of each input parameter on the output (leakage location) was determined by Key Performance Indicator (KPI) and analysis. Figure 4.a shows a listing of KPIs for the leakage location. As it is illustrated in Figure 4.a, skewness (Cum Skewness), standard deviation (Cum ST Dev) and average (Cum Average) of the ΔP are indicated to have the most impact on the output or leakage location. ΔP (Delp) and kurtosis (Cum Kurtosis) follow closely behind. Figure 4.b shows a listing of KPIs for the leakage rate at well D-9-8.

Rank	Feature	% Degree of Influence
1	Cum Skewness(DeltP)	100
2	Cum ST Dev(DeltP)	61
3	Cum Avereage(DeltP)	59
4	Delp	58
5	Cum Kurtosis(DeltP)	50
6	Cum Sum(DeltP)	26
7	Derivitive	2
8	Time(New)	1

Rank	Feature	% Degree of Influence
1	Cum ST Dev(DeltP)	100
2	Delp	86
3	Cum Avereage(DeltP)	75
4	Derivitive	40
5	Cum Sum(DeltP)	36
6	Cum Skewness(DeltP)	5
7	Cum Kurtosis(DeltP)	3
8	Time(New)	1

Figure 4: a) Key performance Indicator for the Leakage Location b) Key performance Indicator for the leakage rate at well D-9-8

It is worth mentioning that descriptive statistics for ΔP data at each time step is calculated on a cumulative basis after pressure threshold of 0.01 psi or leakage indicator is observed. For example, at time step 24 after the pressure threshold was detected, average (Cum Average), summation (Cum Sum), standard deviation (Cum ST Dev), skewness (Cum Skewness) and kurtosis (Cum Kurtosis) were calculated for 24 ΔP records while Derivative and ΔP (Delp) were point values at time step 24. The last 12 data records and corresponding calculated parameters will be used in neural network training.

To validate the performance of the RT-ILDS, a set of blind runs based on data not used for the neural network training were designed, the simulation runs were performed and the appropriate data was collected and pre-processed to an appropriate format for application to the neural network models. As it is shown in Table 1, nine simulation runs were performed considering assignment of three CO_2 leakage rates at the possible locations of the leakage. Pressure signals which corresponded to each CO_2 leakage scenario were processed by applying the leakage threshold of 0.01 psi and generating ΔP, pressure derivative, ΔP average, ΔP summation, ΔP standard deviation, ΔP skewness, and ΔP kurtosis at each time step. The estimated leakage rates for all of the blind runs are summarized in Figure 5.

Table 1: leakage rates and locations for RT-ILDS validation

Run Number	Leakage Rate(ft^3/day)	Leakage Location(ft)	Well
1	23,000	1,268,829	D-9-6
2	72,000	1,268,829	
3	93,000	1,268,829	
4	32,000	1,270,562	D-9-7
5	61,000	1,270,562	
6	87,000	1,270,562	
7	27,000	1,271,495	D-9-8
8	48,000	1,271,495	
9	101,000	1,271,495	

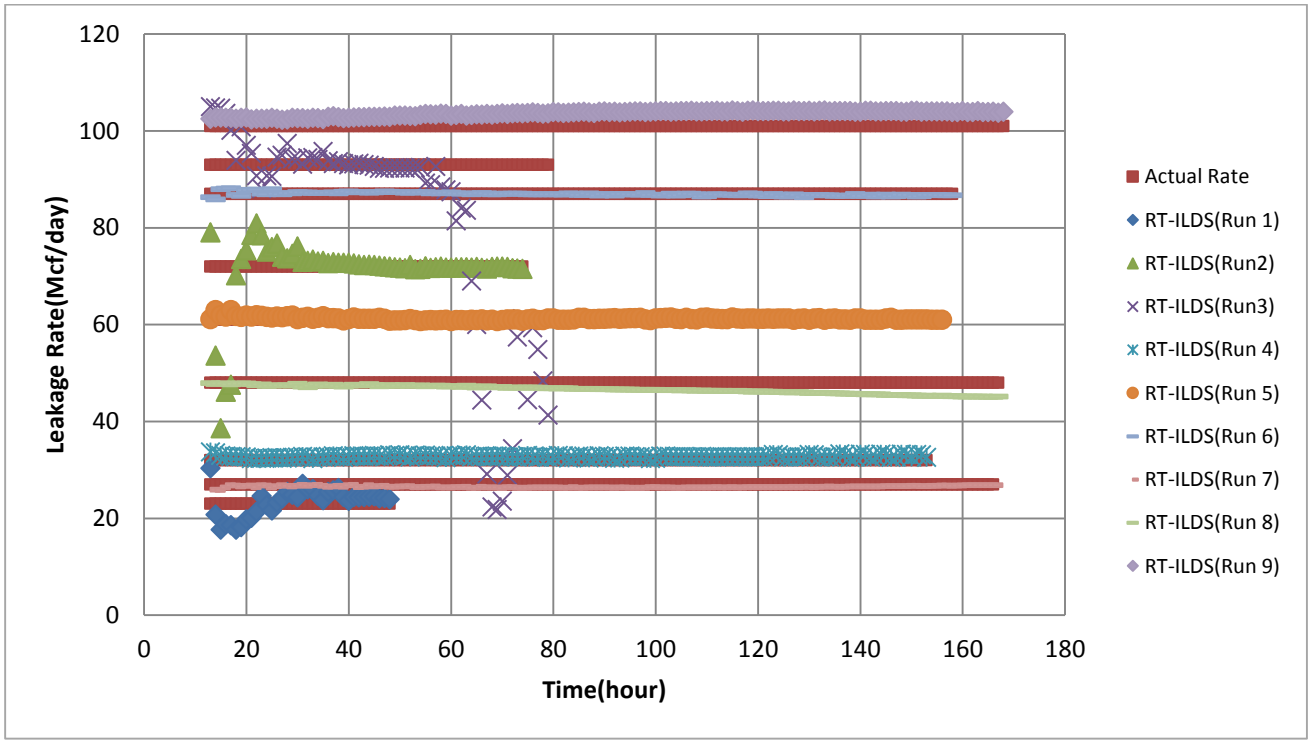

Figure 5: RT-ILDS Leakage rate prediction, all blind runs

Detection Time

When CO_2 leakage occurs in the reservoir (e.g., from existing wells D-9-6, D-9-7, and/or D-9-8), there is a delay before the PDGs receive the generated pressure signal. The time that takes to detect CO_2 leakage depends on the PDG resolution and the amplitude of the pressure signals. The resolution of the PDGs that were installed in observation well is 0.01 psi. Therefore, if the amplitude of a change in the induced pressure signal due to CO_2 leakage is less than the PDG's resolution, the leak will not be detected.

Another parameter related to leakage detection timing is the amplitude of the pressure signal. The signal amplitude is inversely proportional to the distance from the location of the leak to the location of the observation well. The distances from the possible leakage locations at wells D-9-6, D-9-7, and D-9-8 to the observation well are 2366, 746 and 324 ft. respectively. Note that the distance, as far as the transmission of the pressure transients are concerned, includes the impact of the permeability as well as the physical distance between two points. Furthermore, the accuracy of the permeability distribution is a function of the accuracy of the history matching process. . As the leakage location gets closer to observation well, the amplitude of the pressure signal increases. RT-ILDS monitors pressure changes by PDGs with sensitivity of 0.01 psi. Also, the first 12 pressure data records (after detecting a change of ΔP=0.01 psi) were not included in RT-ILDS development. The neural network training results can be improved by ignoring the first 12 pressure data records after the threshold level has been reached and/or exceeded. Based on the mentioned criteria, detection times for different CO_2 leakage rates at each leakage location were plotted in Figure 6. As the distance between the leakage well and the observation well decreases, the pressure signal amplitudes increase and it takes less time to detect the leakage and provide valid results.

RT-ILDS Performance for Multiple Geological Realization

The reservoir simulation model for CO_2 injection at the Citronelle saline aquifer was developed and history matched with real field data. The model acknowledged "lateral heterogeneity" in different ways by considering variable sand layers top, sand thickness, porosity and permeably in the reservoir.

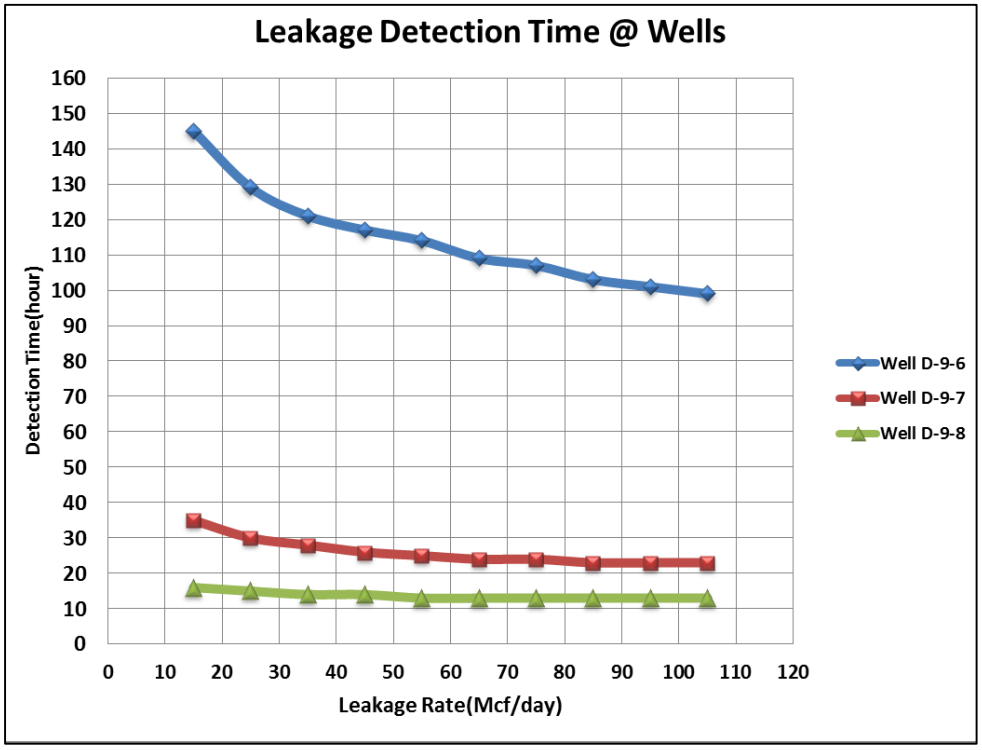

Figure 6: Detection time for each rate at different locations

Multiple reservoir characteristic realizations were generated aimed at changing the parameters that control lateral heterogeneity in the reservoir. Reservoir porosity, sand layer top/thickness and vertical to horizontal permeability ratio were the main parameters to be modified for generating lateral heterogeneity realizations. All these parameters were varied with respect to the original values as illustrated in the Table 2. For each realization, leakage rates equal to 70, 60 and 50 Mcf/day were assigned to wells D-9-6, D-9-7, and D-9-8, respectively.

Table 2: Changes in reservoir properties

Variation / Reservoir Parameter	2% UP	2% low	5% low	10% up	10% low
Porosity				X	X
Sand Layer Top	X	X			
Sand Layer Thickness			X		
Vertical to Horizontal Permeability Ratio				X	

The corresponding pressure signals due to leakage from the wells at the observation well, were collected, processed and fed to the RT-ILDS. It should be mentioned that after changing reservoir characteristics, initial reservoir pressure and stabilization pressure after end of injection varied compare with the initial history matched model. This meant that $P_{No\ Leakage}$ and consequently ΔP had to be recalibrated and recalculated. Pressure signals from different CO_2 leakage rate/location scenarios and reservoir characteristic realizations were collected, processed and fed into the RT-ILDS. The impact of

models specific parameters was studied on the performance of RT-ILDS. For most of the cases, changes in the model parameter did not show significant impact on the RT-ILDS results. The only parameter that considerably impacted RT-ILDS predictions for both CO_2 leakage rate and location was the reservoir porosity. In the reservoir simulation model that was developed for CO_2 injection at the Citronelle field, the reservoir permeability was calculated by porosity-permeability correlation [5]. Therefore, variation of reservoir porosity indirectly changed reservoir permeability. In other words, any change in reservoir porosity led to a change in the permeability as well. Reservoir permeability plays an important role in fluid flow in the reservoir and consequently affects the pressure signals coming from the observation well. The porosity change caused different fluid flow behavior and consequently different pressure signal behavior. As a result, the RT-ILDS results were impacted by variations in the reservoir porosity.

Detection of Leaks at Different Vertical Locations along the Wells

Based on the reservoir simulation results for CO_2 distribution and extension (Figure 7), it was noted that the CO_2 plume reached the existing wells in the reservoir mainly in layer 1. Therefore all the synthetic leakages were assigned to the wells at layer 1 (with the well perforated just in that layer). More investigation showed that CO_2 plume was in contact with well D-9-7 through 9 layers and well D-9-8 in two layers. This means that CO_2 leakage could take place at different vertical locations along the well D-9-7. For that reason, the changes in the vertical leakage location were applied to investigate if the RT-IDLS was capable of detecting the leak and the rate, regardless of the vertical location of the leak within a well.

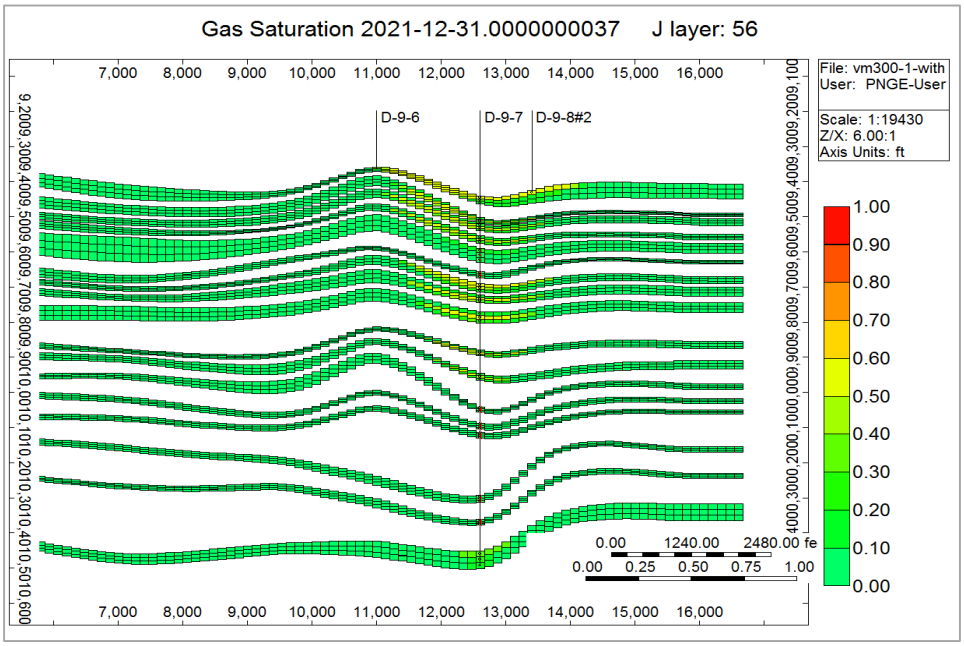

Figure 7: CO_2 plume extension in different layers

Two PDGs were installed at well D-9-8 in the first layer of the reservoir. During the history matching process, based on the reservoir pressure behavior in the observation well, it was concluded that the transmissibility of the shale layers that are inter-bedded in the sand layers was zero [5]. This resulted in no vertical communication between the sand layers. Therefore, if a leak took place at well D-9-7 in layer 5, it would not be possible to observe the pressure change by sensors located in layer 1.

Several PDGs can be installed at the observation well, at multiple sand layers in the reservoir. By including a plurality of PDGs installed in various levels, it is possible to measure pressure changes due to CO_2 leakage at every layer. Therefore, the corresponding pressure changes (ΔP) during potential leakage at well D-9-7 and/or well D-9-8 can be recorded, processed and provided to the RT-ILDS for analysis.

The RT-ILDS results for CO_2 leakage location determination are shown in Figure 8 and leakage rate are shown in Figure 9. Based on the results for leakage location shown in Figure 8, it can be seen that RT-

ILDS is able to detect the CO_2 location correctly when CO_2 leakage took place in well D-9-8 at different vertical locations assuming existence of PDG in every layer. When CO_2 leakage took place at well D-9-7, RT-ILDS correctly determined the leakage location within 80 hours after the leakage except the cases that well leaked form layer 5 and layer twenty nine. 80 hours after the detection time, the results started deviating from actual location of well D-9-7.

A CO_2 leakage rate of 50 Mcf/day was assigned to each leakage scenario at different vertical locations along the well. For the case shown in Figure 9 where well D-9-7 was leaking; the RT-ILDS leakage rate estimations were around 100 Mcf/day. When the leakage was from well D-9-8 at the different layers, the RT-ILDS correctly determined the rate for CO_2 leakage from layer 19. However, the results for CO_2 leakage rate when leak was initiated from layer 5 were not satisfactory. This may be attributed to the pressure signals coming from different layers with completely different reservoir characteristics. Given the variation between layers, the pressure signals will not be exactly the same as the case for CO_2 leakage from layer 1 for which the RT-ILDS was developed and trained.

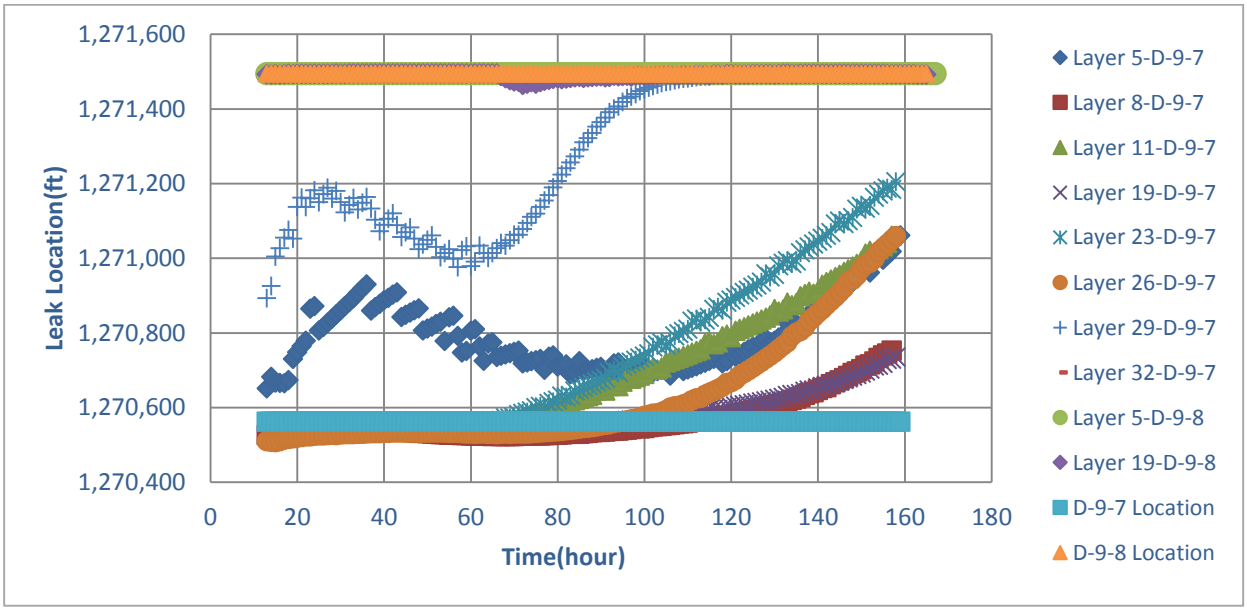

Figure 8; Leakage location prediction; leakage took place at different vertical locations

Effect of Gauge Accuracy or Pressure Drift on RT-ILDS Results

One parameter that affects the accuracy of the pressure measurements is the pressure sensor drift (PSD). Most PDGs experience drift over their life time. PSD can be defined as a gradual malfunction of the sensor that may create offsets in pressure readings from the original calibrated form [14]. Changes in reservoir temperature or pressure can make the PDGs to respond differently depending on the manufacturing characteristics. The scale of PSD changes can vary according to working conditions and manufacturing specifications.

PSD can be measured as how much the pressure readings deviated from the original value in a year (psi/year) or other time period. Different PSD values [12] for the PDGs ranges from 0.25 to 4 psi/year. For RT-ILDS, Pressure Sensor Drift (PSD) can act as a CO_2 leakage indicator. When ΔP of greater than 0.01 is recorded by the pressure sensor, RT-ILDS reports a leakage and starts processing the data to quantify leakage characteristics. For example PSD equal to 1 psi/year generates ΔP =0.01psi, almost 88 hours after the initiation of the drift.

Based on the different values, the times that RT-ILDS mistakenly reports a leakage are illustrated in Figure 10. This leakage is due to PSD and not an actual induced pressure change. PSD trends over 168 hours were generated and applied to RT-ILDS (as a substitute for ΔP caused by actual leakage). The RT-

ILDS estimation results for CO_2 leakage location and rate are shown in Figure 11. RT-ILDS results for the leakage location at early times oscillate between wells D-9-6 and D-9-7. After 80 hours, all the results converge to well D-9-6. This means that PSD makes RT-ILDS to report inaccurately that well D-9-6 is leaking.

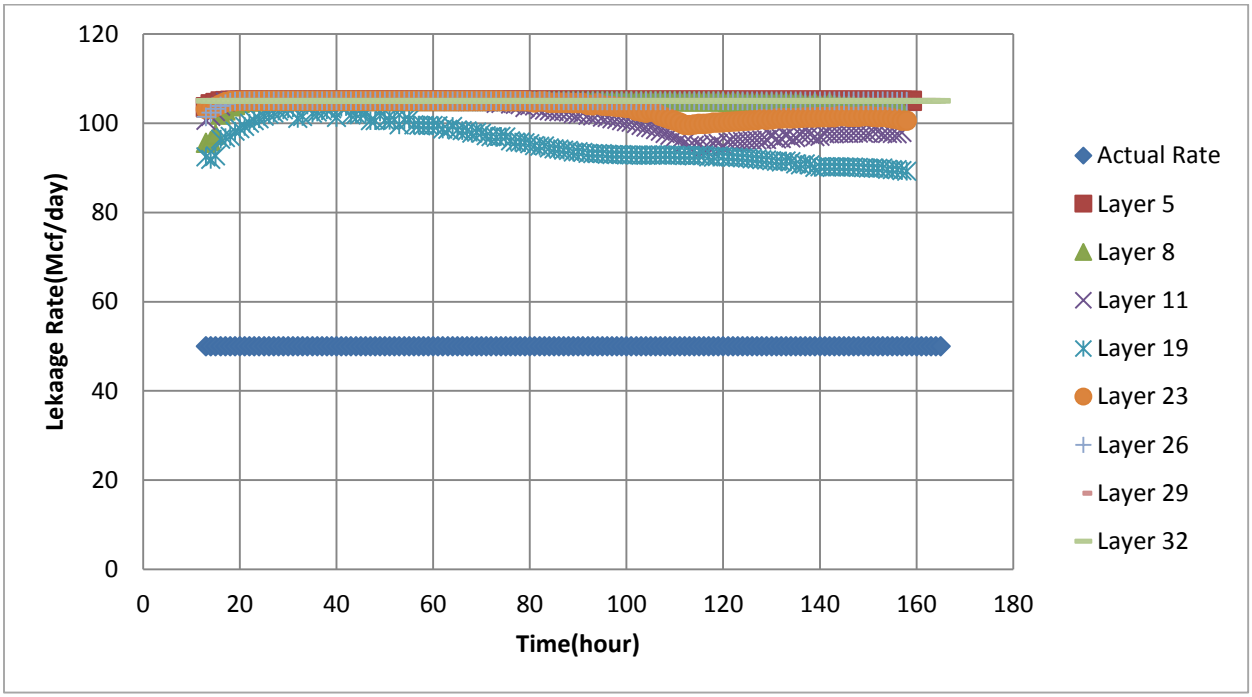

Figure 9: Leakage rate prediction at well D-9-7 when leakage took place at different vertical locations

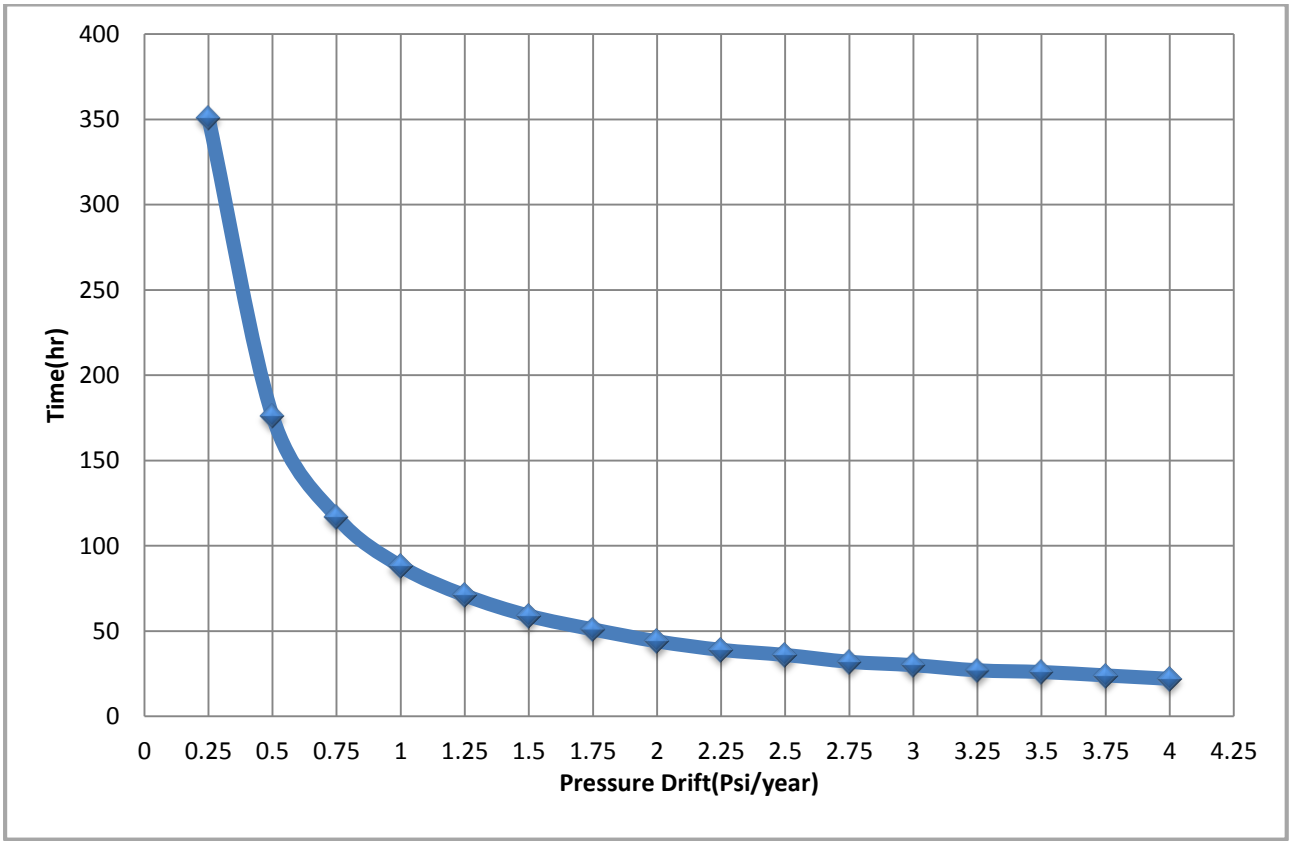

Figure 10: Time to report a false leak based on different PSD values

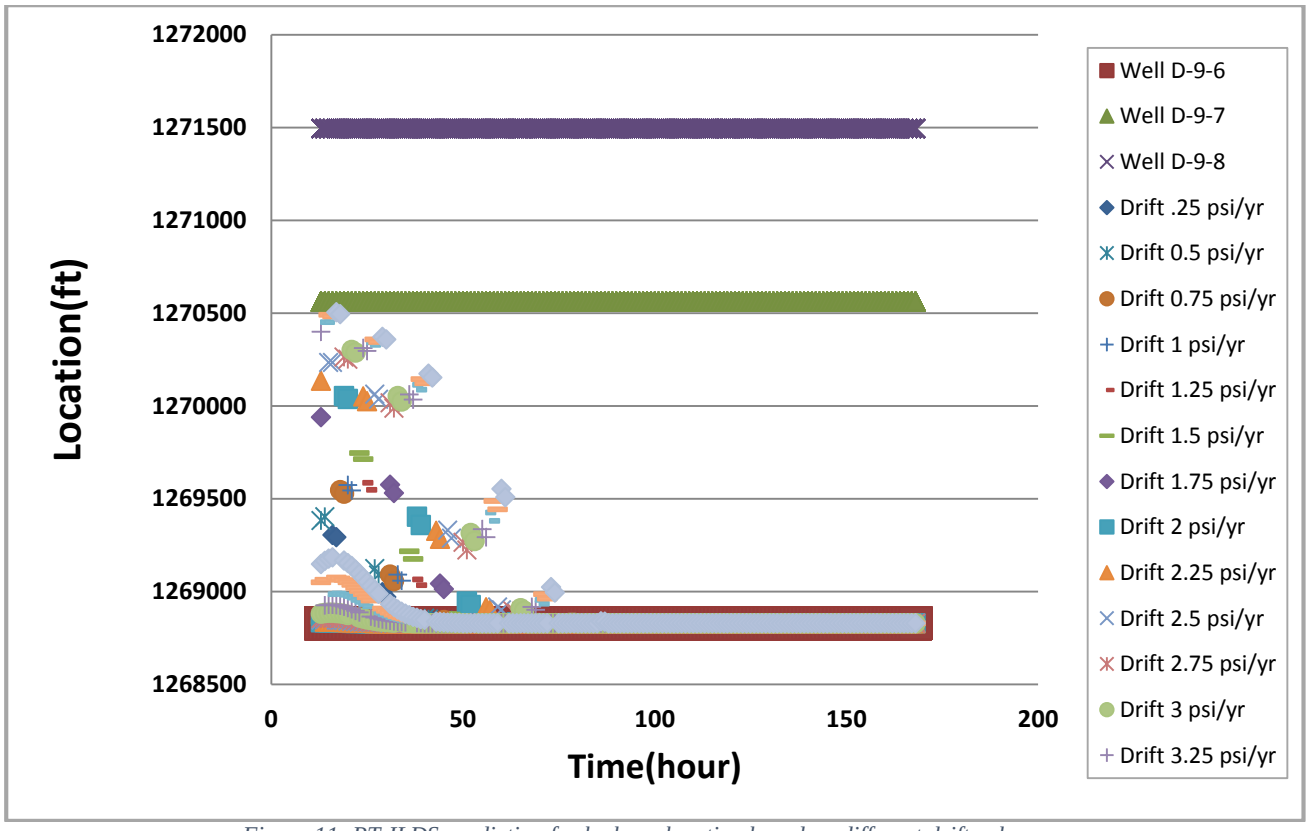

Figure 11: RT-ILDS prediction for leakage location based on different drift values

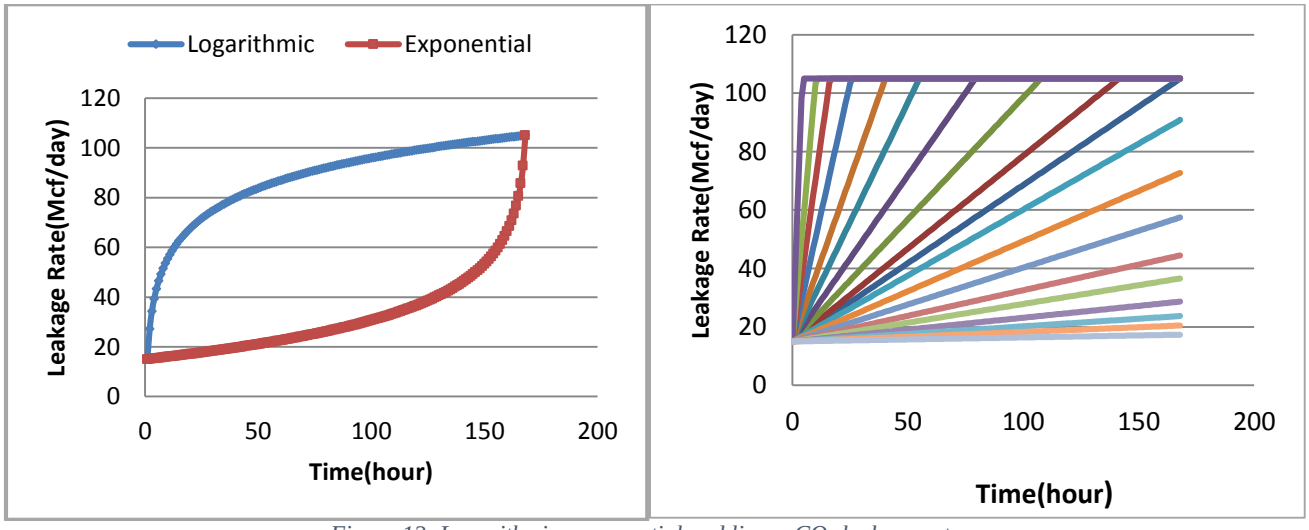

Figure 12: Logarithmic, exponential and linear CO_2 leakage rates

RT-ILDS for Variable CO_2 Leakage Rates

The RT-ILDS is capable of analyzing pressure signals that were generated by CO_2 leakage rates with step function behavior. To simulate the step function behavior, the CO_2 leakages were initiated at a defined rate that remained constant as the time passed. The effects of variable CO_2 leakage rates on the

performance of RT-ILDS were also evaluated using a set of simulation runs designed with different CO_2 leakage rate behaviors including, e.g., linear, exponential and logarithmic changes. The corresponding pressure signals for each variable rate function were included in leakage detection system development. Examples of exponential, logarithmic and linear CO_2 leakage rate functions are shown in Figure 12.

30 different CO_2 leakage rates were assigned to each possible leakage locations; wells D-9-6, D-9-7, and/or D-9-8 in the reservoir simulation model, for 90 total simulation runs. The corresponding pressure signals for each CO_2 leakage scenario were collected, processed and sorted to form a data set for pattern recognition technology. For CO_2 leakage location detection with different leakage rate functions, all of the pressure signals coming from the 90 simulation runs as function of time and their calculated time-based descriptive statistics were lumped together to form the input data set. Therefore, the input data set included 10,950 data records that were partitioned into training, calibration and verification sets based upon the ratios 80%, 10% and 10%, respectively. The outputs for the neural network were the three leakage locations of wells D-9-6, D-9-7, and D-9-8. As in previous situations, the neural network was able to find the pattern between leakage location and pressure signals with high precision ($R^2 = 0.998$). Three neural networks were individually trained for each well to detect the leakage rate. The input data was the same as that used for the leakage location training. However the output was the CO_2 leakage rate at each specific time. The results for CO_2 leakage rate from well D-9-8 are shown in Figure 13. The neural networks were able to determine a pattern between 30 different CO_2 leakage rate functions (as a function of time) and the corresponding pressure signals quite accurately ($R^2 = 0.999$).

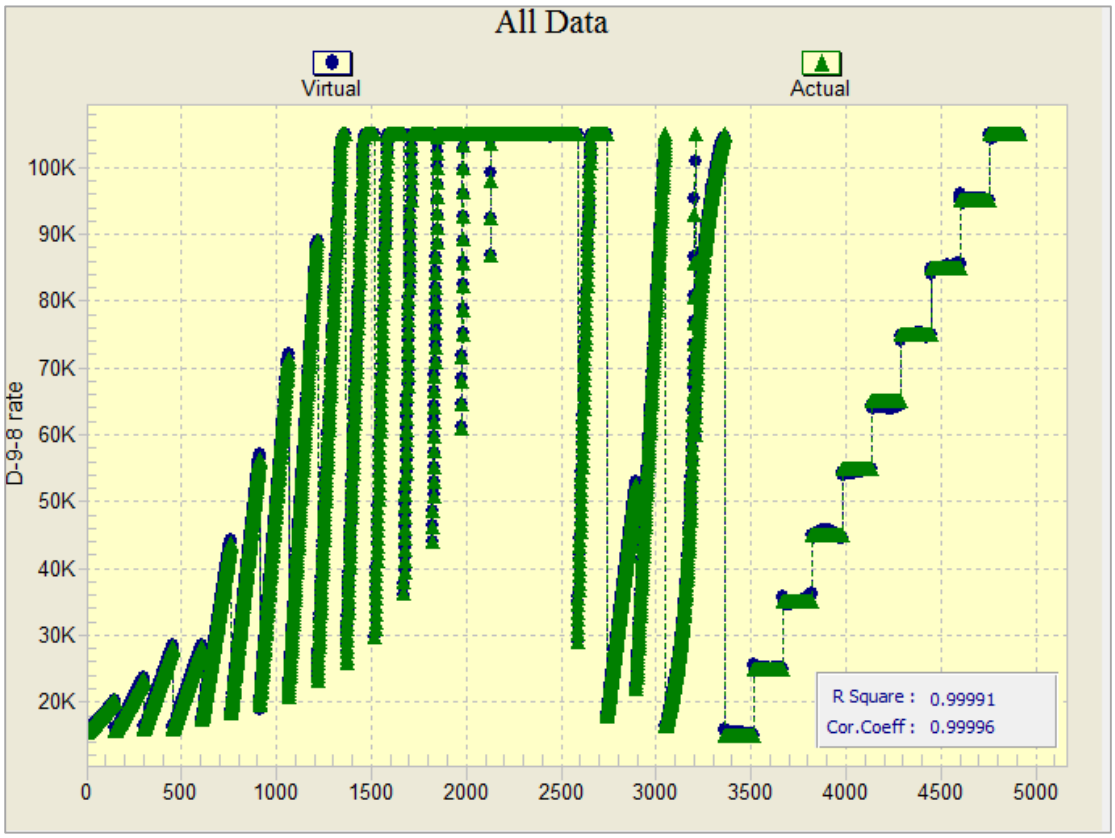

Figure 13: Neural network results for leakage rates at well D-9-8

To further validate the performance of the RT-ILDS, a complex CO_2 leakage rate as a function of time was considered for a blind test. This rate function represented a logarithmic behavior at the beginning followed by a linear trend. The end part of the rate function showed exponential characteristic. The rate function for the blind run is illustrated in Figure 14.a. The rate function was assigned to each of the leakage locations (D-9-6, D-9-7, and D-9-8) as the rate constraints and corresponding pressure signals from the observation well (D-9-8) were collected. The pressure signals were processed to determine real time ΔP

and calculate the descriptive statistics values to be applied to the RT-ILDS. The RT-ILDS estimations for the CO_2 leakage location and leakage rate (at well D-9-8) are shown in Figure 14.b and Figure 15, respectively.

As can be seen in Figure 14.b, the RT-ILDS estimations for the CO_2 leakage locations were reasonably accurate. The RT-ILDS was able to estimate the location of each well correctly. For the CO_2 leakage rate in well D-9-8, the RT-ILDS estimation shown in FIG. 24C represented the actual rate at the early times with reasonable accuracy. RT-ILDS estimated just one value for rate at each time.

In order to have range of rates rather than a single value, "Monte Carlo" simulation was used. Monte Carlo method is a computerized mathematical technique designed for explanation of risk in quantitative analysis and decision making. The following elements illustrate the Monte Carlo simulation process:

- Identification of a range for possible inputs;
- Generation of random inputs from a probability distribution over the range;
- Execution of a large number of simulations with determined inputs; and
- Collection, combination and analysis of the results.

The domain of the input parameters was defined by having Key Performance Indicator (KPI) analysis for leakage rate in Well D-9-8(Figure 4.b).

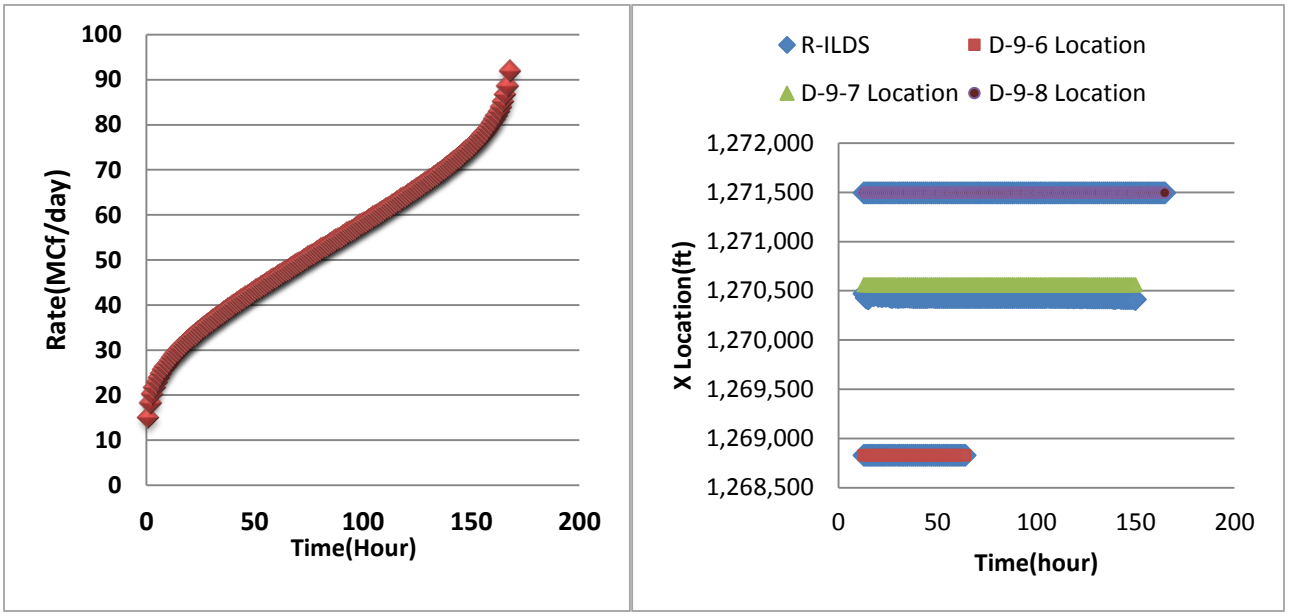

Figure 14: a) Rate function for the blind run *b) RT-ILDS prediction for leakage location (variable rate)*

Cumulative summation ΔP (Cum Sum (DeltP)), average ΔP (Cum Average (DeltP)), standard deviation ΔP (Cum ST (DeltP)), derivative and ΔP indicated the most impact on the CO_2 leakage rate in well D-9-8. Based on a "±20%" rectangular probability distribution, 1000 random variables for each parameter were generated. The trained neural network then computed the CO_2 leakage rate 1000 times based on combinations of the generated input variables. Calculated leakage rates were sorted according to their relative frequency and cumulative probability. Figure 16 shows the relative frequency and cumulative probability for the leakage rate 162 hours after leakage was detected. The actual rate was 83 Mcf/day while RT-ILDS determination indicated 67.4 Mcf/day. As shown in Figure 16, Monte Carlo results provided a leakage rate range that included the actual rate.

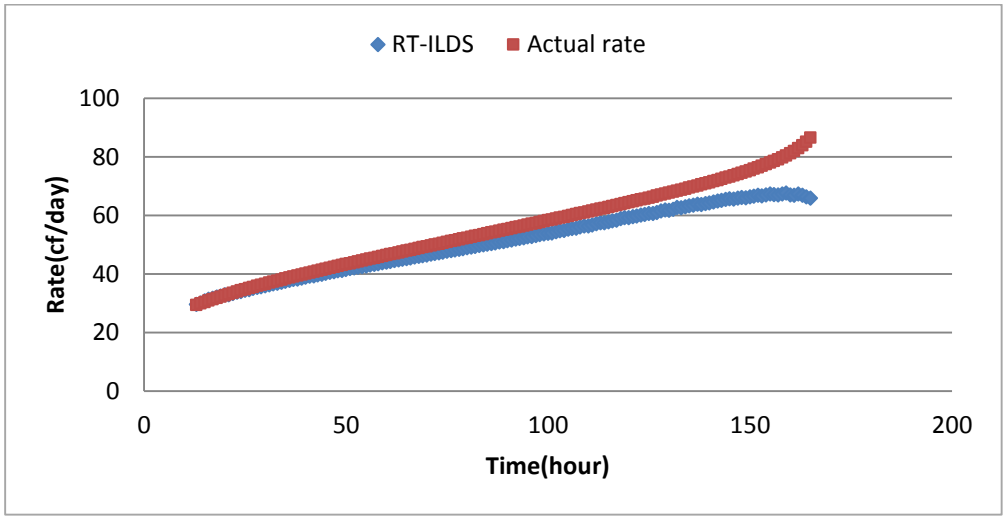

Figure 15: R-ILDS prediction for leakage rate in well D-9-8 (variable rate)

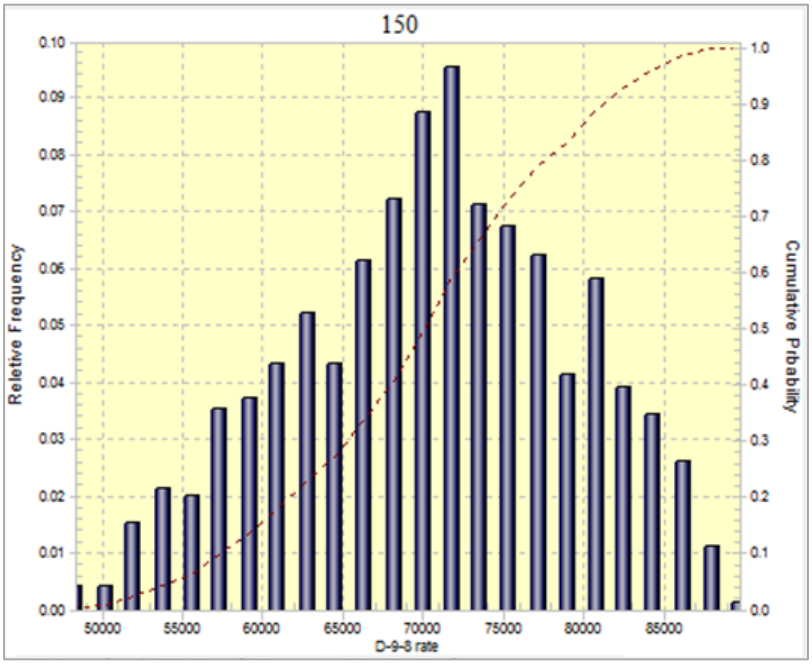

Figure 16: Relative Frequency and cumulative probability for leakage rate (well D-9-8) at time 162hr

Use of PDG in Injection Well

Two PDGs were installed in the well D-9-8#2 to measure and transfer real-time pressure data to the surface. The PDGs can be installed in the injection well (D-9-7#2) rather than in the observation well. This can reduce the need for drilling an observation well. All of the reservoir simulations runs that addressed the 30 different CO_2 leakage scenarios were repeated in order to generate high frequency pressure data at the injection well. The same procedure was used to apply the new sets of data or high frequency pressure data collected at the injection well to the RT-ILDS. According to the training results, the RT-ILDS was able to estimate the CO_2 leakage rates with good precision so that the CO_2 leakage rates' R^2 were more than 0.99 for all three wells, D-9-6, D-9-7, and D-9-8. For the CO_2 leakage location, the RT-ILDS results did not represent the actual locations (CO_2 leakage location R^2 was 0.49). This may be attributed to the injection well having been located approximately in the middle of wells D-9-6 and D-9-

8 as shown in Figure 3.a. As can be seen, the distance between the injection well and the other wells is almost equal.

This symmetric characteristic of the well locations leads to substantially the same pressure signals when either well D-9-6 or D-9-8 leaked. Figure 17 shows a plot of the pressure signals subject to leakage from wells D-9-6 and D-9-8. Since the injection well is located in the middle of CO_2 plume (based on the reservoir characterization), it receives the same pressure signals from different leakages that are at the same distance to the well. Therefore it is not possible to detect the exact location correctly. PDGs should be installed at a location that can provide distinct pressure signals from the different leakage locations. The use of a second monitoring well can enable directional detection of the CO_2 leakage location. For example, directionality may be provided by monitoring PDGs in both the injection and observation wells.

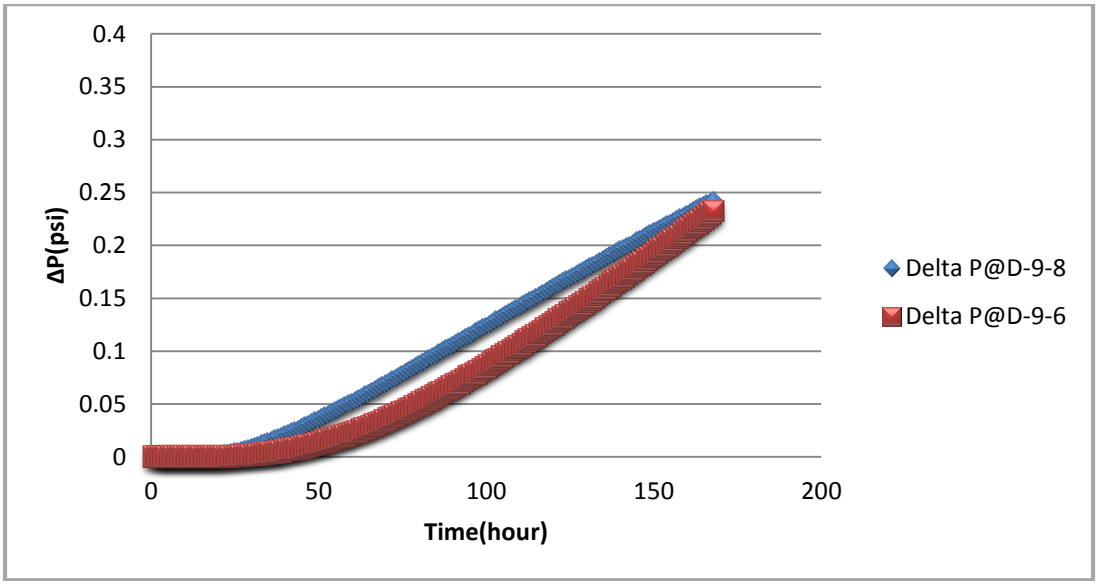

Figure 17: Pressure signals subject to leakages at well D-9-6 and D-9-8

Leakage from Cap Rock

Initially, the reservoir was assumed to have a continuously sealed cap-rock that prevented any communication between the reservoir and formations above it. After the injection period, pressure on one side of the seal (in the target zone) would increase leading to a pressure difference across the cap-rock. When the pressure difference across the cap rock exceeds the fracture pressure, the seal layer can breach and provide a path for CO_2 to migrate to the other layers [15]. In order to model cap-rock leakage in the reservoir simulator, the pressure in the Dantzler sand [11] located on top of the seal was estimated by having the pressure gradient in the formation and its average depth. This pressure was assigned as the constraint for the cap rock leakage in the model. The pressure difference between two layers was assumed to be the main driving force for CO_2 flow through the leakage path.

As an example, consider the reservoir pressure (in the observation well) and CO_2 leakage rate behavior for the case where cap rock leakage occurs north of the injection well. Figure 18.a illustrates the location of the cap rock leakage with respect to the other wells. The pressure behavior in the observation well and CO_2 leakage rate due to cap rock breach is shown in Figure 18.b. When the cap-rock fracture is initiated, a large amount of CO_2 can be released and leaked to the upper layer in a very short period of time (less than a day). This high flow rate of CO_2 leakage causes sharp decline in the reservoir pressure.

As the reservoir pressure decreases, the driving force (pressure difference between reservoir and top sand layer) declines and slows the CO_2 leakage rate. Typically, the pressure signal that is created due to the cap rock leakage represents higher amplitudes when compared with the well leakages signals that were

previously discussed. Therefore a different RT-ILDS implementation was used to detect and quantify the characteristics of cap rock leakage. To develop the RT-ILDS for detecting the cap-rock leakage, nine different simulation runs were designed based on the location of the leakage. FIG. 27C shows the different locations for the cap rock leakage and three blind runs. The only constrain for cap-rock leakage was pressure in the upper layer (Dantzler sand), which was assigned as the bottom-hole pressure for a synthetic well that was drilled in the leakage location.

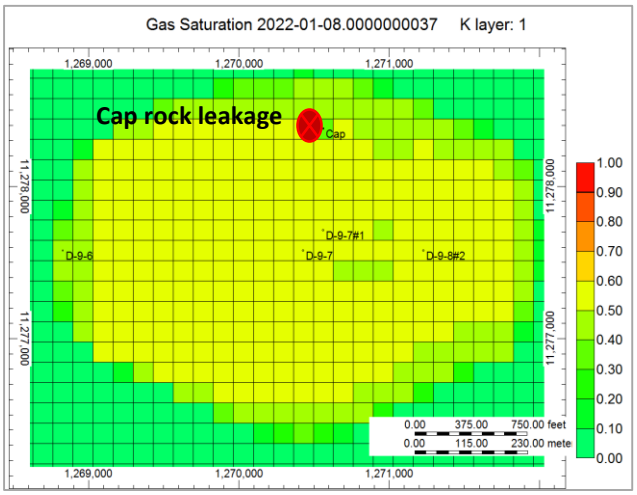

Figure 18: a) Cap-rock leakage location

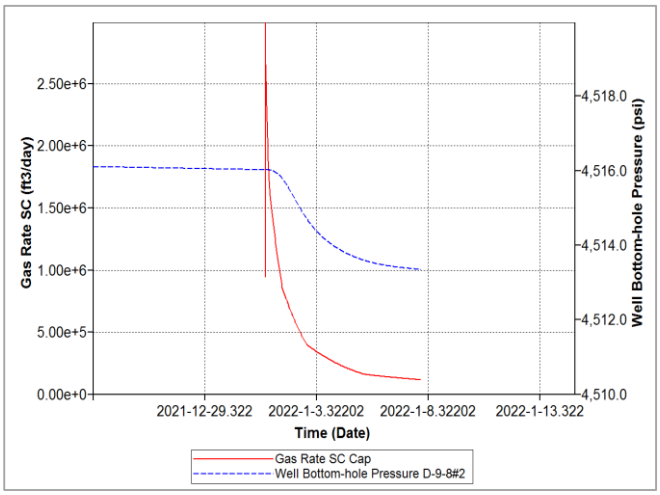

b) Pressure behavior in the observation well and CO_2 rate due to cap rock leakage

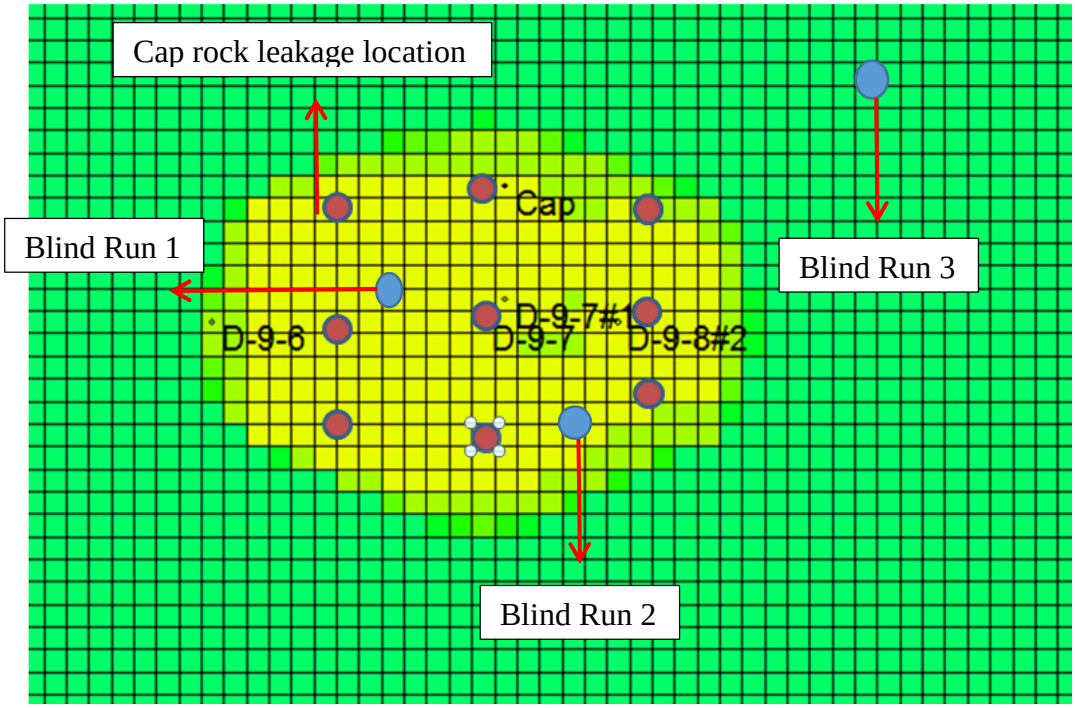

Figure 19: 9 different locations for cap-rock leakages and 3 blind runs

As mentioned earlier, there is a sharp increase in the CO_2 leakage rate. To eliminate this peak in the CO_2 leakage rate behavior, the cumulative amount of leaked CO_2 was used instead of the leakage rate. The training process was the same as previously explained. For each leakage scenario, the corresponding pressure signals were processed in real time by descriptive statistics to be used as the input for the neural

network. The outputs of the neural network were the leakage location (x and y) and the cumulative leaked CO_2. The neural network results for cumulative leaked gas and the x coordinate of the leakage location were precise with R^2 equal to 0.97, and 0.99, respectively. For the y coordinate of the leakage location, the neural network estimations were not as accurate as the x coordinate. This might be attributed to the symmetric locations of cap-rock leakages with respect to the observation well in "y" direction. The final part for the verification of the cap-rock RT-ILDS was to design a set of blind runs that were not used during the neural network training process.

Three cap-rock leakage locations were considered in the reservoir simulation model of Figure 19. Two cap-rock leakage locations (out of three) were inside the range of the locations used for neural network training. For cumulative leaked gas, the RT-ILDS results are almost the same as the actual values for the first two blind run cases, which were located in the range of locations (Figure 20.a). For the third blind run, which was located outside the range, the RT-ILDS results overestimated the actual value considerably (Figure 20.b). X-coordinate results were almost the same as actual locations except blind run 2. For the y coordinate results, there were noticeable differences between actual values and RT-ILDS estimation. Overall, the location of cap-rock leakage can be determined, however it may not be as accurate as well-leakage due to symmetry of the location and the impulsive and uncertain behavior of the leakage.

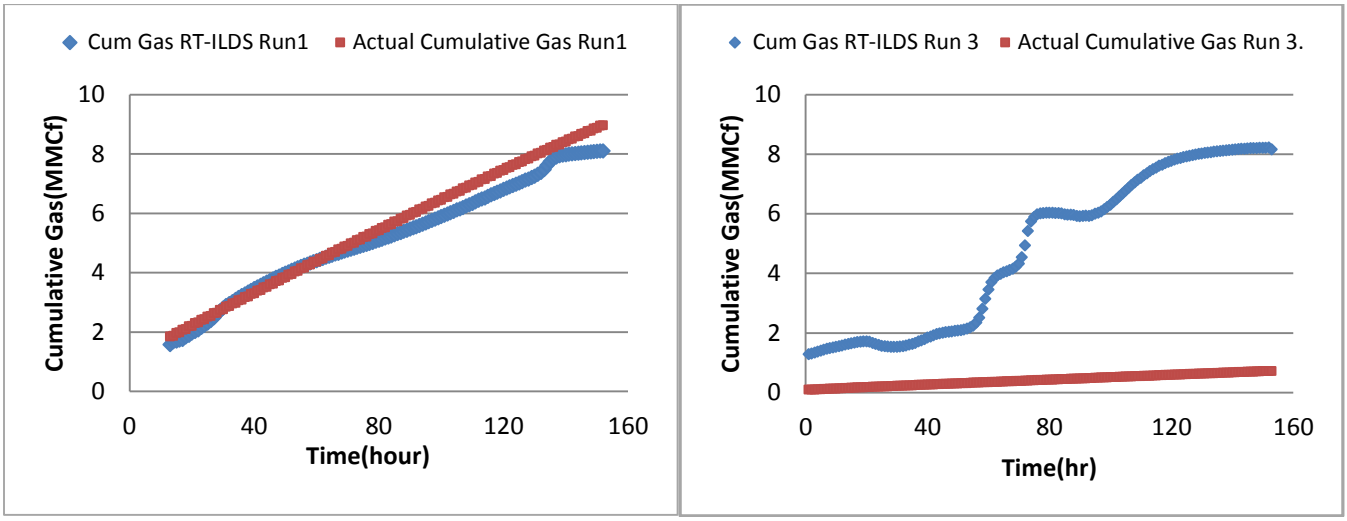

Figure 20: a) R-ILDS prediction for cumulative leaked gas, Blind Run 1 b) R-ILDS prediction for cumulative leaked gas, Blind Run 3

Multi-Well Leakage

Since it is possible for leakage to simultaneously take place at multiple locations, the capabilities of the RT-ILDS to detect multiple leakages was examined. To investigate multi-well leakage, a combination of leakage rates for two and three wells were assigned to the wells in the reservoir model according to Table 5 (Appendix 1). After performing simulation runs based on multi-well leakage scenarios and processing all the corresponding pressure signals, a neural network was trained to differentiate between various combinations of well leakages. In this regard, a "leakage index" was defined based on the distance of each well from the observation well. Longer distances from the observation well resulted in selecting lower values for the leakage index. The index values ranged from 1 to 7, with higher values representing higher pressure signal amplitude) according to distance to the observation well and the number of the leaking wells. All the scenarios can be divided into three classes as: single well leakages (indices: 1, 2, and 3), two well leakages (indices: 4, 5, and 6) and three well leakage (index: 7). the leakage index values are shown in Table 3.

Several neural networks were trained considering different leakage indices as the output and processed pressure signals (ΔP) as the input. The convolution of several pressure signals generated by different

combinations of well leakages makes it very difficult for the neural networks to catch specific patterns out of final pressure signals. In order to de-convolve mixed pressure signals (generated by multi-well leakages), existence of an additional PDG was considered in the injection well in addition to the observation well. Only two well leakages were subject to investigation (leakage index values of 4, 5, and 6). The addition of one more PDG provided more information about pressure signals and the time that signals were observed by the PDGs. For this case, a neural network was trained using a generalized regression neural network (GRNN) algorithm. The results for neural network training are shown in Figure 21.

Table 3: Leakage Index for different single and multi-well leakage scenarios

Table 4: CO2 leakage rates for the blind runs-two well leakages

Run	Two Well Leakage Rate(Mcf/day)			Leakage Index
	D-9-6	D-9-7	D-9-8	
1	40	80	0	4
2	80	40	0	4
3	40	0	80	5
4	80	0	40	5
5	0	40	80	6
6	0	80	40	6

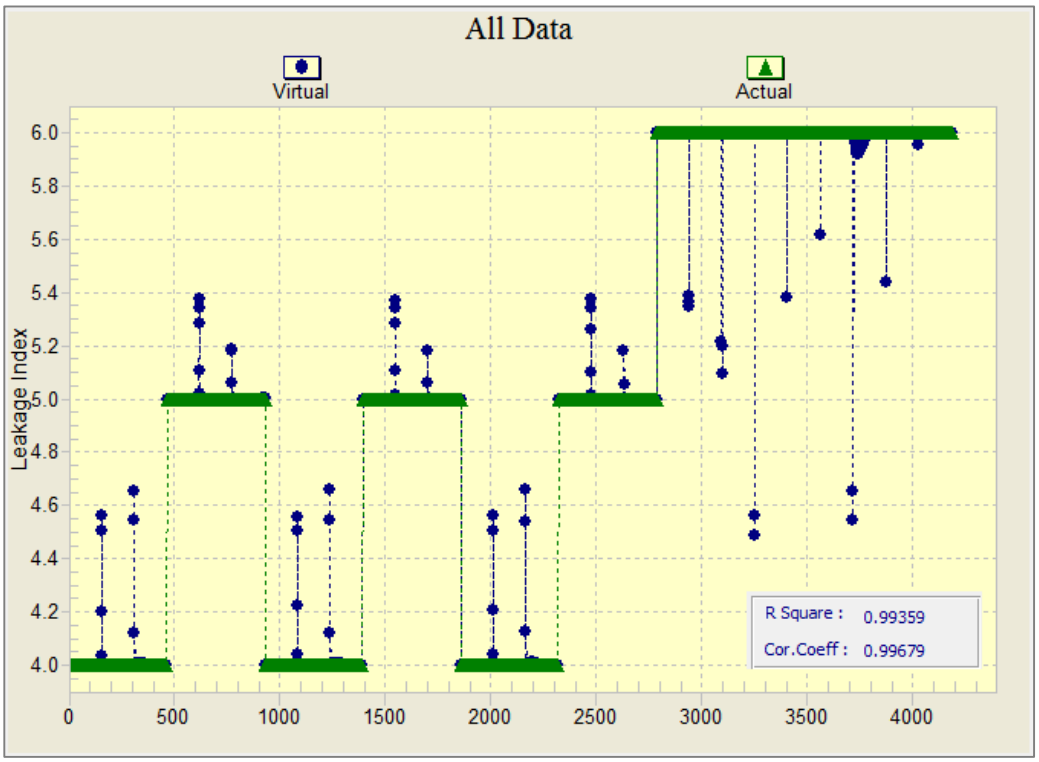

Figure 21: generalized regression neural network (GRNN) results for two-well leakage

By adding more PDGs in the injection well, the results for neural network training improved significantly (R^2 equal to 0.9935). As a result, it became possible to differentiate which two wells were leaking by having pressure signals coming from two pressure down-hole gauges. The final step was to

verity the practicality of the RT-ILDS which was devolved for multi-well leakage. To do so, six simulation runs considering combinations of two-well leakages were performed. Table 4 summarizes the CO_2 leakage rates for the two well blind runs. The results for blind run verifications are shown in Figure 22. RT-ILDS was able to estimate the leakage index correctly except for a few hours immediately after the leakages. Although the probability of two wells leaking simultaneously is low, the use of PDGs installed in two distinct wells makes it possible to distinguish which wells are leaking at the same time.

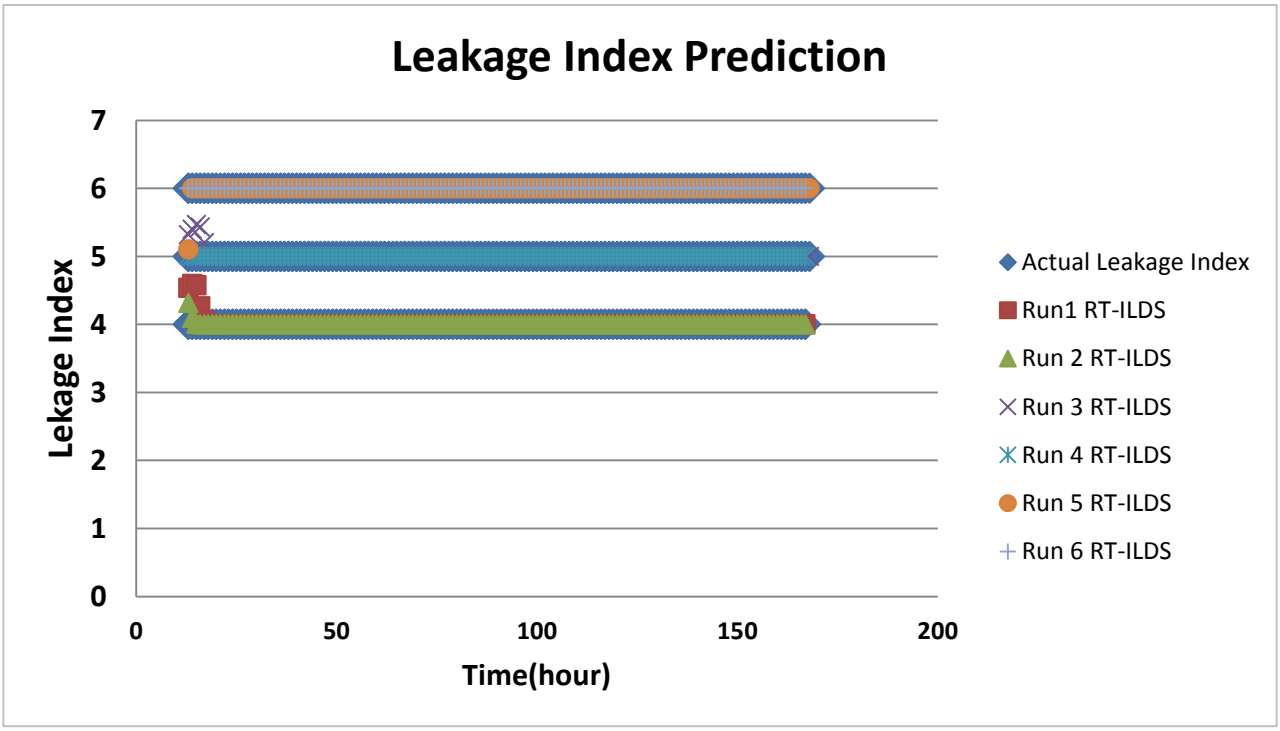

Figure 22: RT-ILDS predictions for two-well leakages

Conclusions

In this work, a comprehensive study was performed to improve RT-ILDS capabilities and test it over different uncertain parameters. Verified and history matched model was used for CO_2 leakage modeling.

- At the beginning, a new data processing method was proposed to make ILDS to a fast responsive and real time detection tool (RT-ILDS). CO_2 leakage characteristics (amount and location) were determined much faster that what was proposed [?] by RT-ILDS. Additionally, minimum detection times for RT-ILDS subject to various leakage locations and rates were determined by considering pressure behavior at observation well and resolution of the PDG. Closer the leaking well to the observation well and higher the leakage rates represented shorter time for leakage detection.
- 4 different reservoir parameters as porosity, sand layer top, sand layer thickness and vertical to horizontal permeability ratio were varied to investigate their effect on the RT-ILDS predictions. Change of reservoir porosity showed to have higher impacts on R-ILDS results especially for CO_2 leakage location and some cases leakage rate predictions. Sand layer top was the other important parameter that impacted RT-ILDS results.
- The ability of RT-ILDS was tested to see if it was possible to detect leakages that took place at different vertical locations along the wells. It was observed that with current locations of the PDGs (first sand layer) it would not be possible to sense any pressure changes due to leakage

in other layers. Due to presence of impermeable shale layers between the sands that caused no inter communications between layers; PDG should be installed at each layer specifically, to be able to detect leakages at different vertical locations.

- The effect of Pressure Sensor Drifts (PSD) was studied on performance of the RT-ILDS. According to different reported values for PSDs, the time that RT-ILDS reported a leakage (false leakage) and predicted leakage locations were determined. Within the range of pressure drifts (0.25 to 4 psi/year), it took from 20 to 350 hours that RT-ILDS report a leakage. Additionally, RT-ILDS predicted that leakage took place mostly at well D-9-6.
- The ability of detecting leakages with variable CO_2 leakage rates was added to RT-ILDS. To do so, multiple CO_2 leakage rates with linear, exponential and logarithmic behavior were assigned to leakage locations. Corresponding pressure signals were used to train a new neural network. RT-ILDS represented good results and was tested successfully with a blind run. Besides that, RT-ILDS demonstrated distribution by use of Monte Carlo simulation for predicted CO_2 leakage rates.
- The possibility of using injection well as the monitoring well was investigated as part of this work. Injection well RT-ILDS predicted the leakage rates with high accuracy but failed to predict the location of leaking wells due to the symmetric locations of leaking wells respect to injection well.
- Cap-rock fractures provide a conduit for CO_2 to leak of the target formations. Cap-rock leakage behavior (release high amount of CO_2 in very short time) was different from well –leakage and was modeled separately in the simulation model considering the cap-rock thickness and reservoir pressure in the overlaying sand layer. Nine possible locations of Cap-rock leakage were proposed within the CO_2 plume extension. RT-ILDS was re-developed and verified based on pressure signals coming from 9 simulation and 3 blind runs. RT-ILDS predictions were within a reasonable range for cumulative leaked gas and x- coordinate of leakage location.
- The final concern for RT-ILDS was the ability of detecting multi-well leakages. Fifty four simulation runs were performed with two-well and three-well leaking scenarios. With just one observation well, it was not possible to distinguish different leakage scenarios. Addition of one more observation well in the location of injection well, enabled RT-ILDS to find which two wells leak simultaneously.

Acknowledgment

Authors would like to acknowledge Advanced Resources International (ARI), US DOE, EPRI, and SSEB for providing the field data, Computer Modeling Group for providing the reservoir modeling /simulation software CMG-GEM™ and Intelligent Solutions, Inc. (ISI) for providing the IDEA™ software (which was used for data driven analysis) for the case study that were conducted at PEARL group at West Virginia University.

References

[1] Birkholzer, J., Nicot, J., Oldenburg, C., Zhou, Q., Kraemer, S. and Bandilla, K. "Brine flow up a well caused by pressure perturbation from geologic car-bon sequestration: static and dynamic evaluations," Int. J. Greenh. Gas Con, no. 5, pp. 850-861, 2011.

[2] Celia, M., Nordbotten, J., Court, B., Dobossy, M., and Bachu, S., "Field-scale application of a semi-analytical model for estimation of CO2and brine leakage along old wells," Int. J. Greenh. Gas Con, no. 5, pp. 257-269, 2011.

[3] Cooper, C., A Technical Basis for Carbon Dioxide Storage, CO2 Capture Project, 2009

[4] Haghighat, S.A., Mohaghegh, S. D., Borzouie, N., Moreno and, D., Shahkarami, A., "Reservoir Simulation of CO2 Sequestration in Deep Saline Reservoir, Citronelle Dome, USA," in Twelfth Annual Conference on Carbon Capture, Utilization and Sequestration., Pittsburgh, 2013
[5] Haghighat, S. A., Mohaghegh, S. D, Gholami, V. and Shahkarami, A., "Pressure History Matching for CO2 Storage in Saline Aquifers: Case Study for Citronelle Dome," in Carbon Management Technology Conference, Alexandria, 2013.
[6] Haghighat, S. A, Mohaghegh, S. D, Gholami, V., Shahkarami, A. and Moreno, D., "Using Big Data and Smart Field Technology for Detecting Leakage in a CO2 Storage Project," in SPE Annual Technical Conference and Exhibition, New Orleans, 2013.
[7] Jalali, J. "Artificial Neural Networks for Reservoir Level Detection of CO2 Seepage Location Using Permanent Down-Hole Pressure Data," West Virginia University, Morgantown, 2010.
[8] Jung, Y., Quanlin, Z., and Birkholzer J., "Early detection of brine and CO2 leakage through abandoned wells using pressure and surface-deformation monitoring data: concept and demonstration." Adv. Water Resources, 2011
[9] Koperna G.J, Kuuskraa V.A.,Reistenberg D.E, Rhudy R., Trautz R., Hill G.,Esposito R.A," The SECARB Anthropogenic Test: The First US Integrated Capture, Transportation, and Storage Test" Carbon Management Technology Conference, 7-9 February 2012, Orlando, Florida, USA
[10] Kuuskraa V.A.," Cost-Effective Remediation Strategies for Storing CO2 in Geologic Formations", SPE International Conference on CO2 Capture, Storage, and Utilization, 2-4 November 2009, San Diego, California, USA, 2009
[11] Petrusak R, SPE, Cyphers S., SPE, Bumgardner S, SPE, Advanced Resources International; Hills D, Pashin J., Geological Survey of Alabama; Esposito R, Southern Company**,** Saline Reservoir Storage in an Active Oil Field: Extracting Maximum Value From Existing Data for Initial Site Characterization; Southeast Regional Carbon Sequestration Partnership (SECARB) Phase III**,** SPE International Conference on CO2 Capture, Storage, and Utilization, 10-12 November 2010, New Orleans, Louisiana, USA
[12] Reiter, J., Murphy, D. and Larson, N., "Drift Measurements in Pressure Sensors," in Ocean Sciences Meeting, Salt Lake City, 2012.
[13] Sun, A., "Inversion of pressure anomaly data for detecting leakage at geologic carbon sequestration sites," Advances in Water Resources, vol. 56, pp. 49-60, 2013.
[14] Solinst, "Solinst Canada Ltd,", [Online]. Available: http://www.solinst.com/products/dataloggers-and-telemetry/3001-levelogger-series/technical-bulletins/understanding-pressure-sensor-drift.php. [Accessed 2013].
[15] Tran, D., Shrivastava, V. K., Nghiem, L. X., Kohse, B. F.," Geomechanical Risk Mitigation for CO2 Sequestration in Saline Aquifers", SPE-125167-MS, SPE Annual Technical Conference and Exhibition, 4-7 October 2009, New Orleans, Louisiana.
[16] Zeidouni, M., and Pooladi-Darvish, M., "Characterization of Leakage through Cap-Rock with Application to CO2 Storage in Aquifers - Single Injector and Single Monitoring Well," in Canadian Unconventional Resources and International Petroleum Conference, Calgary, 2010.

Appendix 1

Table 5: CO_2 leakage rates for multi-well leakage

Two Well			Three Well		
Leakage Rate(Mcf/day)			Leakage rate(Mcf/day)		
D-9-6	D-9-7	D-9-8	D-9-6	D-9-7	D-9-8
15	15	0	15	15	15
15	60	0	15	15	60
15	105	0	15	15	105
60	15	0	15	60	15
60	60	0	15	60	60
60	105	0	15	60	105
105	15	0	15	105	15
105	60	0	15	105	60
105	105	0	15	105	105
15	0	15	60	15	15
15	0	60	60	15	60
15	0	105	60	15	105
60	0	15	60	60	15
60	0	60	60	60	60
60	0	105	60	60	105
105	0	15	60	105	15
105	0	60	60	105	60
105	0	105	60	105	105
0	15	15	105	15	15
0	15	60	105	15	60
0	15	105	105	15	105
0	60	15	105	60	15
0	60	60	105	60	60
0	60	105	105	60	105
0	105	15	105	105	15
0	105	60	105	105	60
0	105	105	105	105	105